Super-Resolution MRI Synthesis Using a GAN Framework

Veeresh S Hiremath[0009−0003−1983−8460],
Manoj Pandekamat[0009−0004−1728−7324],
Rahul Pujari[0009−0003−8654−8551],
Neha[0009−0000−6322−1474],
Sumaiya Pathan[0009−0000−6931−7661]

School of Computer Science and Engineering,
KLE Technological University - Hubballi, India
01fe22bcs296, 01fe22bcs279, 01fe22bcs286, 01fe22bcs327,
sumaiya.pathan@kletech.ac.in

Abstract. Magnetic Resonance Imaging (MRI) is a vital diagnostic tool in medical imaging, but acquiring high-resolution MRI scans will be time-consuming, expensive, and uncomfortable for patients. X-rays emit ionizing radiation that can damage DNA and potentially cause cancer. Although a single scan carries minimal risk, repeated or high-dose exposure—especially in children—raises long-term cancer risk. Limited research on reconstructing high-quality images from low-resolution including the blur inputs, super-resolution models often overfit to specific MRI types or body regions (e.g., brain MRI only) and perform poorly on unseen systems or anatomical structures this resulting in loss of anatomical accuracy, poor generalizability across MRI modalities, and instability during training. To address these challenges, this paper proposes a Generative Adversarial Network (GAN)-based approach for MRI super-resolution that reconstructs high-quality 256x256 grayscale images from low-resolution 128x128 inputs. The architecture integrates a deep convolutional generator and discriminator trained adversarially to learn fine details and enhance image fidelity. The preprocessed MRI datasets, and the model was evaluated using Peak Signal-to-Noise Ratio (PSNR), Structural Similarity Index (SSIM), Visual Assessment, Mean Squared Error (MSE), Pixel Accuracy, Perceptual loss. The GAN-based model generated sharper and more detailed MRI images, effectively restoring tissue structures and reducing blurriness. Quantitative metrics showed improved SSIM up to 0.866, PSNR up to 29.24 dB, and reduced MSE with the accuracy of 97.79%. These results demonstrate the model's strength for enhancing diagnostic imaging where high-resolution scans are limited.

Keywords: MRI, DNA, resolution, GAN, PNSR, SSIM

1 INTRODUCTION

Deep learning has demonstrated exceptional abilities in complicated data-driven tasks and has been widely utilized across areas, including healthcare and agriculture [1–5]. These developments provide a strong basis for investigating generative AI techniques centered on data synthesis and simulation.

Magnetic Resonance Imaging plays a pressing role in medical diagnostics, offering non-invasive and detailed imaging of soft tissues such as the brain, muscles, and organs [6]. High-resolution MRI scans are essential for accurate disease detection, treatment planning, and monitoring of conditions like tumors, neurological disorders, and vascular anomalies [7]. However, acquiring high-resolution MRI images is often limited by long scanning times, patient discomfort, and hardware constraints. These limitations not only affect clinical workflows but can also compromise diagnostic precision in time-sensitive cases [8, 9].

To address these challenges, MRI super-resolution techniques aim to reconstruct high-resolution images from low-resolution inputs, thereby improving image quality without increasing scan time [10]. Traditional interpolation-based methods like bicubic or spline interpolation often result in blurred and less accurate reconstructions [11]. In recent years, the emergence of deep learning—particularly Convolutional Neural Networks and Generative Adversarial Networks has revolutionized image super-resolution by learning complex patterns and textures directly from data [12, 13].

Super-resolution in MRI presents unique challenges, such as preserving anatomical structure, avoiding artifacts, and dealing with highly sparse or noisy input data [14]. While CNNs have shown notable improvements, GAN-based methods offer superior perceptual quality by incorporating adversarial loss and generating more realistic textures [15, 16]. However, training GANs is complex due to issues like mode collapse, instability, and overfitting on small medical datasets [17].

Despite these hurdles, recent research demonstrates that GAN-based models can significantly improve resolution and fidelity of MRI images, making them suitable for clinical and research applications [18]. Effective super-resolution can enhance diagnosis accuracy, reduce the need for repeat scans, and enable earlier detection of critical conditions. Given the high demand for fast and accurate imaging, intelligent SR methods are essential in modern healthcare settings [19, 20].

The main goal of this project is to explore,implement a GAN-based super-resolution model for MRI, converting low-resolution grayscale inputs 128x128 into high-resolution outputs 256x256. By comparing the proposed model with conventional methods like Interpolation methods, Multi-image Super-Resolution, Iterative Back-Projection, Regularization-Based methods this study seeks to identify the most reliable approach for enhancing image quality while maintaining anatomical accuracy.

The subsequent sections provide a detailed review of related work, focusing on the prevailing challenges in 5G network security. Section 2 presents a literature survey, examining existing methodologies and their suitability for intrusion detection. Section 3 outlines the proposed methodology, highlighting the pro-

posed GAN model for image super-resolution. Section 4 summarizes the results in a tabular format, showcasing the evaluation of model and speaks about future scope. Finally, Section 5 concludes the findings, offering insights drawn from the results and suggesting directions for future work. The paper ends with an acknowledgment of contribution.

2 Literature Review

High-resolution MR images are vital for precise diagnosis but are slow to acquire, while low-resolution images are faster but lack detail. The conditional GAN with perceptual loss to super-resolve LR MRI scans, combining adversarial and perceptual losses for realistic and anatomically accurate results [21]. Their model outperforms existing methods, proving effective for both isotropic and anisotropic super-resolution, as confirmed by quantitative evaluations. By conditioning on LR inputs, the approach ensures clinically viable HR outputs without prolonged scan times [22].

FA-GAN introduces a fused attentive GAN for MRI super-resolution, combining multi-scale feature extraction with channel and self-attention mechanisms to enhance diagnostic-quality HR images from LR scans [23]. The model employs spectral normalization to stabilize training and a Local Fusion Feature Block to preserve fine anatomical details, outperforming traditional methods in PSNR and SSIM metrics. The integration of attention mechanisms ensures superior feature focus, improving spatial relationships in reconstructed images [23]. This advancement makes high-resolution MRI more accessible for time-sensitive diagnoses without compromising accuracy.

A lightweight 3D Multi-Level DenseNet-GAN (mDCSRN-GAN) for efficient MRI super-resolution, achieving 4x upscaling while maintaining computational speed and anatomical accuracy [15]. The model's innovative dense connections preserve low-level features often lost in traditional networks, enhancing detail in reconstructed HR images [24]. Trained on 1,113 subjects, it outperforms existing methods in both quality and efficiency, addressing critical SNR and scan-time limitations in clinical MRI, by combining 3D feature extraction with adversarial training, it generates realistic outputs suitable for time-sensitive diagnostics [24].

SOUP-GAN introduces a 3D perceptual GAN for medical super-resolution, combining multi-scale architecture with 3D patch-based perceptual loss to enhance thin-slice MRI/CT reconstruction. The two-stage training MSE initialization + GAN refinement preserves textures better than single-scale methods, generalizing across modalities like brain/knee MRI and CT. By processing $32\times32\times3$D patches from diverse datasets (BraTS, LIDC-IDRI), it reduces aliasing while improving edge sharpness at variable sampling factors. Quantitative results show superiority over interpolation methods, particularly in structural clarity for cross-sectional views (axial/coronal/sagittal).

SSimDCL introduces a GAN-based framework that simultaneously enhances MRI resolution and segmentation accuracy, outperforming CycleGAN and other methods in brain tissue/tumor boundary detection. By combining supervised

learning with adversarial training, it achieves superior performance in FID, KID, PSNR and Dice metrics compared to state-of-the-art techniques. The model's patch-based NCE loss and identity preservation improve detail retention when upscaling both normal and high-resolution MRI datasets [15, 21]. Clinical validation shows its effectiveness for VolBrain-comparable segmentation while generating diagnostically useful high resolution outputs [15].

DC-GAN and WGAN to address medical imaging dataset limitations by generating high-quality synthetic MRI scans that preserve structural integrity. WGAN emerges as superior to DC-GAN, producing more realistic outputs with higher PSNR and SSIM scores while maintaining training stability [25]. By strategically eliminating style transfer and aggregation steps that degraded image quality, the approach focuses on pure GAN-based augmentation for optimal results [22]. The method effectively enhances dataset diversity for deep learning models, particularly valuable for rare conditions or imbalanced classes [25].

3 Proposed Work

This section explains the methodology to create the MRI super-resolution model, starting from data preprocessing, normalization, and continuing with the model preparation and execution that uses Machine learning and deep learning (Scikit-learn and TensorFlow, respectively), data analysis, and visualization (NumPy, Pandas, Seaborn, andMatplotlib). The dataset used in this study is the MRI ND5 [26] dataset mixed with other MRI images of body parts, which is a widely recognized benchmark dataset for MRI super resolution, representing real-world MRI images from variety of the body-parts [27]. The High resolution images 512x512, 256x256 and 128x128 forms are shown in Figures 1a and 1b, respectively.

The dataset mainly consists the images of various resolution but most of them are with the resolution of 512x512, so instead of converting all of them to the same using the methods of the augmentation we have dropped the images which are other than the required 512x512 image resolution. Then on the filtered images we have prepared the dataset where we have used the techniques of the resizing and converting them to the 256x256 high res images and 128x128 low res images the low res images are automatically the blur is applied when the resizing is used also we have used the techniques like guaissian blur for the proper blurring of the images.

The proposed image super-resolution framework utilizes a lightweight Generative Adversarial Network (GAN) architecture specifically designed to upscale grayscale low-resolution medical images from 128×128 to 256×256. The generator network is built on a residual convolutional backbone that initiates with a Conv2D layer comprising 64 filters and ReLU activation, followed by four residual blocks, each containing two convolutional layers with skip connections. This residual design enhances feature learning and gradient flow, which is crucial for preserving structural integrity in high-resolution outputs. An upsampling block utilizing nearest-neighbor interpolation followed by convolution ensures $2\times$ spa-

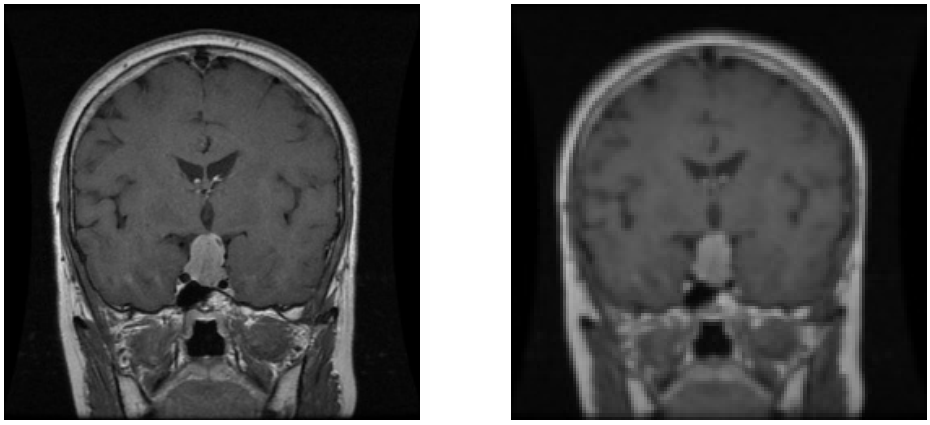

(a) 256x256 image quality in dataset (b) 128x128 image quality in dataset

Fig. 1: Comparison of high and low resolution image from prepared dataset

tial resolution enhancement. The generator concludes with a sigmoid activation to produce normalized output. The Fig 3 represents the architecture of the proposed GAN.

The discriminator is a fully convolutional binary classifier that takes a 256×256 image and outputs a probability score indicating its authenticity. It comprises three convolutional layers with LeakyReLU activations and stride-based downsampling, followed by a flattening operation and a sigmoid-activated dense layer. The adversarial loss is modeled using binary cross-entropy, while content similarity is preserved using a Mean Squared Error (MSE) loss between the generated and real high-resolution images. The model is optimized using Adam optimizers with distinct learning rates for the generator (1e-4) and discriminator (1e-5), stabilizing the GAN convergence over 10 epochs with a batch size of 8.

Generator Network: Let the low-resolution MRI image be denoted by $I_{LR} \in \mathbb{R}^{H \times W}$, where H and W are the height and width of the image. The generator G aims to produce a high-resolution version $\hat{I}_{HR}$ as shown in Eq 1:

$$\hat{I}_{HR} = G(I_{LR}; \theta_G) \tag{1}$$

Where θ_G represents the learnable parameters of the generator network.

Discriminator Network: The discriminator D attempts to distinguish between real HR images I_{HR} and generated images $\hat{I}_{HR}$. Its output is given by Eq 2:

$$D(x) = \sigma(f(x; \theta_D)) \tag{2}$$

Fig. 2: Original high resolution image from the dataset

Where $x \in \{I_{HR}, \hat{I}_{HR}\}$, f is the internal computation of the discriminator, σ is the sigmoid activation, and θ_D are the discriminator parameters.

Adversarial Loss: The adversarial loss for the generator, encouraging it to produce outputs indistinguishable from real HR images, is given by Eq 3:

$$\mathcal{L}_{adv} = -\log(D(G(I_{LR}))) \tag{3}$$

Perceptual Loss: To ensure perceptual similarity, the generated image is compared with the real HR image using a feature extractor ϕ, such as a pretrained VGG network. The perceptual loss is defined in Eq 4:

$$\mathcal{L}_{perc} = \sum_{l=1}^{L} \|\phi_l(I_{HR}) - \phi_l(\hat{I}_{HR})\|_2^2 \tag{4}$$

Where ϕ_l is the activation from the l-th layer of the feature extractor.

Total Generator Loss: The total loss for training the generator combines adversarial and perceptual loss, as shown in Eq 5:

$$\mathcal{L}_G = \lambda_{adv}\mathcal{L}_{adv} + \lambda_{perc}\mathcal{L}_{perc} \tag{5}$$

Where λ_{adv} and λ_{perc} are weighting factors to balance the two losses.

Discriminator Loss: The discriminator is trained using the binary cross-entropy loss to correctly classify real and fake images, given in Eq 6:

$$\mathcal{L}_D = -\log(D(I_{HR})) - \log(1 - D(G(I_{LR}))) \tag{6}$$

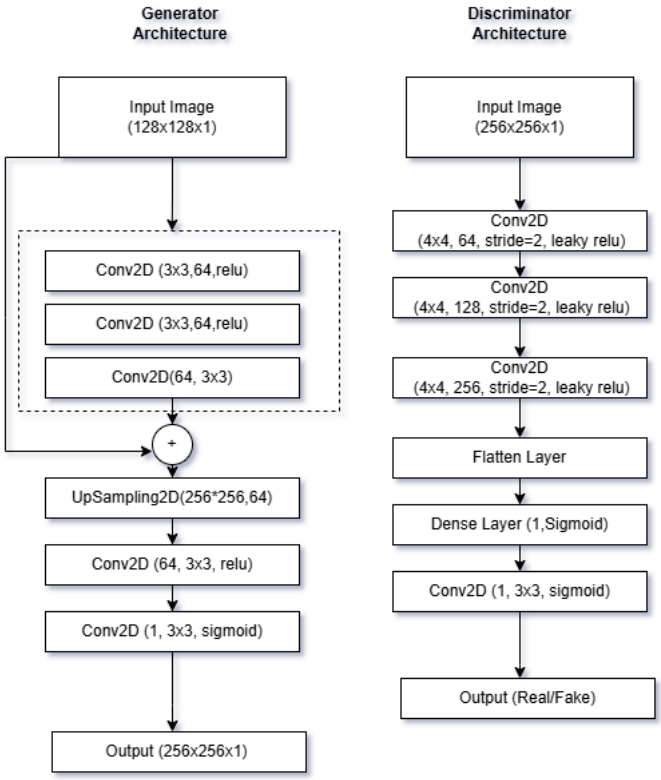

Fig. 3: GAN architecture

Final Output: The super-resolved image output by the trained cGAN generator is in Eq7:

$$I_{SR} = G(I_{LR}) \tag{7}$$

This I_{SR} is visually high quality and structurally faithful, usable for clinical MRI diagnosis.

The algorithm 1 explains about the training and the working method of the GAN model.

The images of the dataset are classified as the tumor positive and negative images by the pretrained model for getting the images separately which are tumor positive. The GAN model build by us is tested against this positive and generalized images for comparison in the super-resolution for the infected and non-infected patients MRI images.

Algorithm 1: Testing Process for Image Super-Resolution using GAN

Require: Low-resolution image $I_{\text{LR}} \in \mathbb{R}^{H \times W}$, Trained Generator G_{θ_G}, optionally trained Discriminator D_{θ_D}

Ensure: Super-resolved image $I_{\text{SR}} \in \mathbb{R}^{sH \times sW}$

Step 1: Preprocessing
Normalize input I_{LR} to range $[0, 1]$ or $[-1, 1]$ depending on G_{θ_G} input constraints.

Step 2: Forward Pass Through Generator
Compute the super-resolved output:

$$I_{\text{SR}} = G_{\theta_G}(I_{\text{LR}})$$

Step 3: Postprocessing
Clamp or scale I_{SR} pixel values to valid range.
If required, apply denormalization:

$$I'_{\text{SR}} = \text{clip}(I_{\text{SR}} \cdot \sigma + \mu, 0, 255)$$

Step 4 (Optional): Quality Evaluation
if Ground-truth HR image I_{HR} is available **then**
    Compute Peak Signal-to-Noise Ratio (PSNR):

$$\text{PSNR} = 10 \cdot \log_{10} \left(\frac{L^2}{\frac{1}{N} \sum_{i=1}^{N} (I_{\text{HR}}^{(i)} - I_{\text{SR}}^{(i)})^2} \right)$$

    where L is the dynamic range of pixel values and N is the number of pixels.
    Compute Structural Similarity Index (SSIM):

$$\text{SSIM}(I_{\text{HR}}, I_{\text{SR}}) = \frac{(2\mu_{\text{HR}}\mu_{\text{SR}} + c_1)(2\sigma_{\text{HR,SR}} + c_2)}{(\mu_{\text{HR}}^2 + \mu_{\text{SR}}^2 + c_1)(\sigma_{\text{HR}}^2 + \sigma_{\text{SR}}^2 + c_2)}$$

end if
Step 5 (Optional): Adversarial Score
if Discriminator D_{θ_D} is used at inference **then**
    Compute confidence score from the discriminator:

$$\hat{y} = D_{\theta_D}(I_{\text{SR}})$$

    where $\hat{y} \in [0, 1]$ indicates the realism of I_{SR}
end if
return I_{SR} as the super-resolved image output.

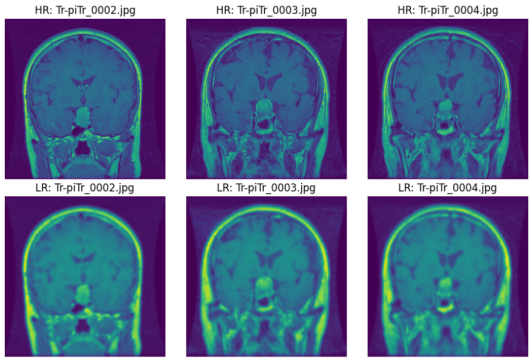

Fig. 4: Pair of high and low resolution images for training

4 Result and Discussion

The proposed GAN-based MRI super-resolution model was trained on a dataset of 1500 grayscale image pairs, each consisting of a 128×128 low-resolution input and a corresponding 256×256 high-resolution target. Training was performed over 100 epochs, during which the model demonstrated consistent improvement in perceptual and quantitative quality. The generator was trained using a composite loss function defined as Eq 8

$$\mathcal{L}_{\text{gen}} = \mathcal{L}_{\text{MSE}} + \lambda \cdot \mathcal{L}_{\text{adv}}, \quad \lambda = 10^{-3} \tag{8}$$

, balancing pixel-level reconstruction with adversarial realism. By the final epoch, the generator achieved a mean loss of 0.0020, the discriminator stabilized at a loss of 1.2450, and the model reached an accuracy of 97.86%.

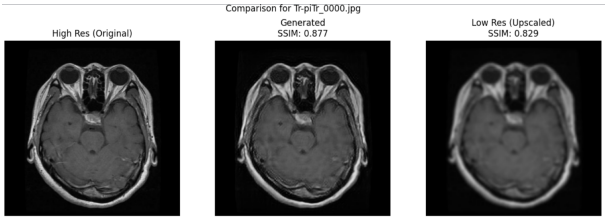

Fig. 5: Original high resolution image from the dataset

Visual inspection in Fig5 confirmed that the model produced sharper, more detailed outputs, successfully recovering tissue structures and reducing blurriness commonly seen in interpolated low-resolution images. The Structural Similarity Index and PSNR values as 0.838(general MRI images), 0.866(for positive) and 29.24db (general) and 27.5 db(positive), respectively are shown in Fig 6a and

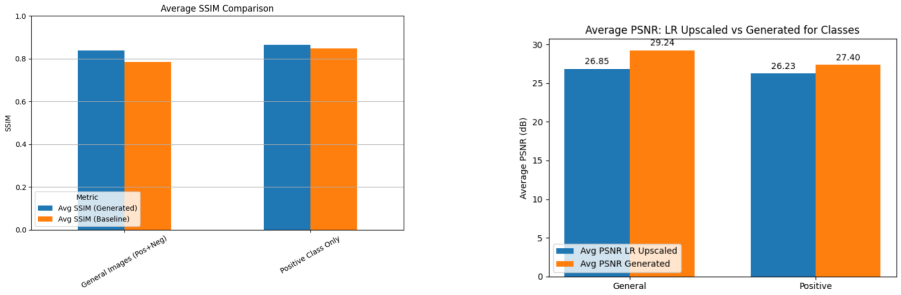

(a) SSIM Comparison (b) PNSR Comparison

Fig. 6: Comparison of high and low resolution results

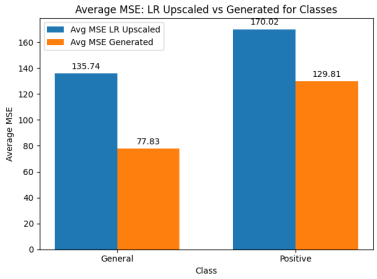

Fig. 7: MSE for the General and Positive class

Fig 6b. Fig 7 represents the MSE for the generated and low resolution images against the original images. This performance underscores the effectiveness of using a GAN framework for medical image super-resolution and highlights its potential utility improving resolution in diagnostic imaging environments where native high-resolution scanning is constrained by acquisition time or equipment limitations.

5 Conclusion and Future Scope

The results of this study demonstrate that the proposed GAN-based model effectively enhances the resolution of MRI scans, achieving a pixel accuracy of 97.86% , average SSIM of 0.866, average PNSR of 27.4 over 100 epochs of training. The model efficiently learns to map low-resolution grayscale MRIs to high-resolution versions using a loss function that combines MSE and adversarial components. Visual evaluation confirms that the network restores fine anatomical structures with significant clarity and realism. These findings affirm the potential of GANs in the field of medical image enhancement, particularly for improving the diagnostic quality of MRI scans acquired under limited-resolution settings.

While the current implementation shows strong performance, several areas for future work remain. First, the model can be extended to operate on 3D

volumetric MRI data to better capture spatial continuity across slices. Furthermore, testing the architecture on multiple MRI modalities (T1, T2, FLAIR) can evaluate its generalizability. To reduce computational load and enable real-time deployment in clinical settings, lightweight variants such as MobileGAN or model pruning techniques may be explored. Additionally, integrating perceptual loss and SSIM-based metrics could further improve texture fidelity. Finally, the model's robustness should be validated on larger, diverse clinical datasets, and extended to unsupervised domain adaptation for broader applicability across imaging centers with varied acquisition protocols.

References

1. S. K. Shiragudikar, G. Bharamagoudar, K. K. Manohara, et al. Insight analysis of deep learning and a conventional standardized evaluation system for assessing rice crop's susceptibility to salt stress during the seedling stage. *SN Computer Science*, 4:262, 2023.
2. S. Y. Malathi, G. R. Bharamagoudar, and S. K. Shiragudikar. Diagnosing and grading knee osteoarthritis from x-ray images using deep neural angular extreme learning machine. *Proceedings of the Indian National Science Academy*, 91:95–108, 2025.
3. S. K. Shiragudikar, G. Bharamagoudar, M. K. K., M. S. Y., and G. S. Totad. Predicting salinity resistance of rice at the seedling stage: An evaluation of transfer learning methods. In *Intelligent Systems in Computing and Communication (ISCComm 2023)*, volume 2231 of *Communications in Computer and Information Science (CCIS)*. Springer, Cham, 2025.
4. S. Pathan, P. Kumar, R. M. Pai, and S. V. Bhandary. Automated segmentation and classification of retinal features for glaucoma diagnosis. *Biomedical Signal Processing and Control*, 63:102244, 2021.
5. S. Pathan, P. Kumar, R. M. Pai, and S. V. Bhandary. An automated classification framework for glaucoma detection in fundus images using ensemble of dynamic selection methods. *Progress in Artificial Intelligence*, 12(3):287–301, 2023.
6. R. F. Kilcoyne, M. L. Richardson, B. A. Porter, D. O. Olson, T. K. Greenlee, and W. Lanzer. Magnetic resonance imaging of soft tissue masses. *Clinical Orthopaedics and Related Research*, 228:13–19, Mar 1988.
7. Xiaohui Li, Chengfang Liu, Lin Zhu, Meng Wang, Yukai Liu, Shuo Li, Qiwen Deng, and Junshan Zhou. The role of high-resolution magnetic resonance imaging in cerebrovascular disease: A narrative review. *Brain Sciences*, 13(4):677, 2023. Review.
8. Hiroyuki Kabasawa. Mr imaging in the 21st century: Technical innovation over the first two decades. *Magnetic Resonance in Medical Sciences*, 21(1):71–82, 2022. Review.
9. Kawin Setsompop, David A Feinberg, and Jonathan R Polimeni. Rapid brain mri acquisition techniques at ultra-high fields. *NMR in Biomedicine*, 29(9):1198–1221, Sep 2016. Review.
10. M. L. de Leeuw den Bouter, G. Ippolito, T. P. A. O'Reilly, R. F. Remis, M. B. van Gijzen, and A. G. Webb. Deep learning-based single image super-resolution for low-field mr brain images. *Scientific Reports*, 12(1):6362, 2022.

11. James Grover, Paul Liu, Bin Dong, Shanshan Shan, Brendan Whelan, Paul Keall, and David E J Waddington. Super-resolution neural networks improve the spatiotemporal resolution of adaptive mri-guided radiation therapy. *Communications Medicine*, 4(1):64, 2024.
12. Junhyeok Lee, Woojin Jung, Seungwook Yang, Jung Hyun Park, Inpyeong Hwang, Jin Wook Chung, Seung Hong Choi, and Kyu Sung Choi. Deep learning-based super-resolution and denoising algorithm improves reliability of dynamic contrast-enhanced mri in diffuse glioma. *Scientific Reports*, 14(1):25349, 2024.
13. Hu Su, Ying Li, Yifan Xu, Xiang Fu, and Song Liu. A review of deep-learning-based super-resolution: From methods to applications. *Pattern Recogn.*, 157(C), January 2025.
14. Diana L Giraldo, Hamza Khan, Gustavo Pineda, Zhihua Liang, Alfonso Lozano-Castillo, Bart Van Wijmeersch, Henry C Woodruff, Philippe Lambin, Eduardo Romero, Liesbet M Peeters, and Jan Sijbers. Perceptual super-resolution in multiple sclerosis mri. *Frontiers in Neuroscience*, 18:1473132, 2024.
15. Hongtao Zhang, Yuki Shinomiya, and Shinichi Yoshida. 3d mri reconstruction based on 2d generative adversarial network super-resolution. *Sensors*, 21(9):2978, 2021.
16. Sarah Oraby, Ahmed Emran, Basel El-Saghir, and Saeed Mohsen. Hybrid of dsr-gan and cnn for alzheimer disease detection based on mri images. *Scientific Reports*, 15(1):12727, 2025.
17. Youssef Skandarani, Pierre-Marc Jodoin, and Alain Lalande. Gans for medical image synthesis: An empirical study. *Journal of Imaging*, 9(3):69, 2023.
18. Waqar Ahmad, Hazrat Ali, Zubair Shah, and Shoaib Azmat. A new generative adversarial network for medical images super resolution. *Scientific Reports*, 12(1):9533, 2022.
19. Jiachuan He, He Ma, Miaoran Guo, Jiaqi Wang, Zhongqing Wang, and Guoguang Fan. Research into super-resolution in medical imaging from 2000 to 2023: bibliometric analysis and visualization. *Quantitative Imaging in Medicine and Surgery*, 14(7):5109–5130, 2024.
20. Minwoo Shin, Minjee Seo, Kyunghyun Lee, and Kyungho Yoon. Super-resolution techniques for biomedical applications and challenges. *Biomedical Engineering Letters*, 14(3):465–496, 2024.
21. K. Zhang, H. Hu, K. Philbrick, et al. SOUP-GAN: Super-resolution MRI using generative adversarial networks. *Tomography*, 8(2):905–919, March 2022. Published 2022 Mar 24.
22. Sahar Almahfouz Nasser, Saqib Shamsi, Valay Bundele, Bhavesh Garg, and Amit Sethi. Perceptual cgan for mri super-resolution, 2022.
23. Mingfeng Jiang, Minghao Zhi, Liying Wei, Xiaocheng Yang, Jucheng Zhang, Yongming Li, Pin Wang, Jiahao Huang, and Guang Yang. FA-GAN: Fused attentive generative adversarial networks for MRI image super-resolution. *arXiv preprint arXiv:2108.03920*, 2021.
24. Yuhua Chen, Anthony G. Christodoulou, Zhengwei Zhou, Feng Shi, Yibin Xie, and Debiao Li. MRI super-resolution with GAN and 3D multi-level densenet: Smaller, faster, and better. *arXiv preprint arXiv:2003.01217*, 2020.
25. Nisa Sarı, Abdullah Elewi, and Mehmet Acı. Image generation performance analysis: A comparative study of gan models on mnist dataset. In *2024 8th International Artificial Intelligence and Data Processing Symposium (IDAP)*, pages 1–7, 2024.
26. Shailja, Nishant, Shilpi Gupta, and Deepti Mehrotra. Brain mri - nd 5 dataset. `https://ieee-dataport.org/documents/brain-mri-nd-5-dataset`, 2020. Accessed: 2025-06-03.

27. Canadian Institute for Cybersecurity. About the canadian institute for cybersecurity, 2024. Accessed: 2024-12-30.